Supplemental data:

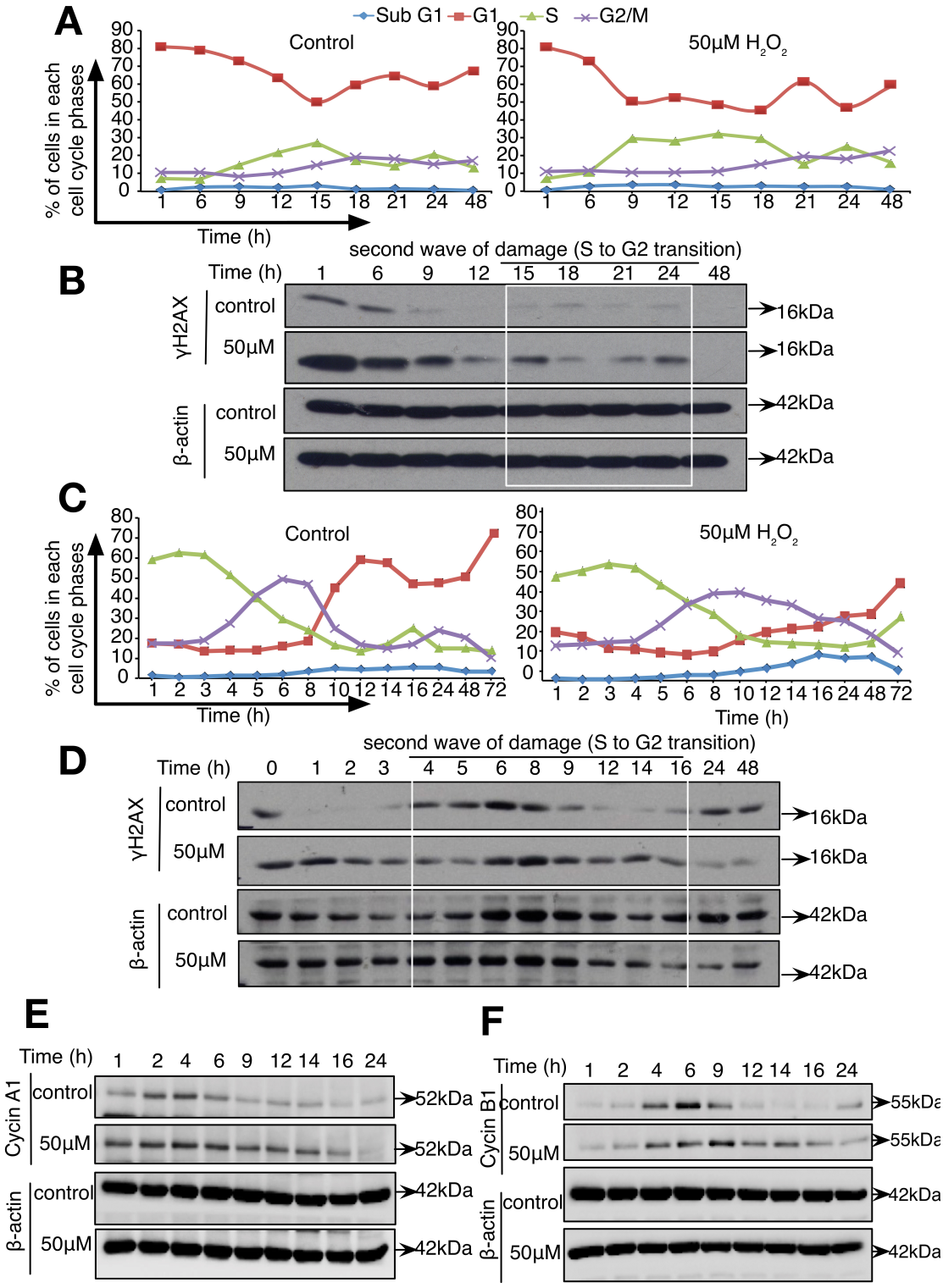

Supplementary Figure 1. Two waves of DNA damage were observed using lovastatin and aphidicolin synchronized L6 cells treated with 50μM H_2O_2.
L6 cells were synchronized using lovastatin or aphidicolin before being treated with 50μM H_2O_2 for 1H and cell cycle and γH2AX profile monitored at the indicated time. (A) Line plots capturing the percentage of cells in each phase at indicated time points in control and 50μM H_2O_2 treated cells by synchronizing the cells using lovastatin. The cell population gating was fixed across all time points based on the non-

synchronized cell population. (B) Western blot showing γH2AX phosphorylation in the lovastatin-synchronized untreated and 50μM H_2O_2 treated cells. (C) Line plots capturing the percentage of cells in each phase at indicated time points in control and 50μM H_2O_2 treated cells by synchronizing the cells using aphidicolin. The cell population gating was fixed across all time points based on the non-synchronized cell population. (D) Western blot showing γH2AX phosphorylation in the aphidicolin-synchronized untreated and 50μM H_2O_2 treated cells. (E) Western blot showing the expression pattern of cyclin A1 in untreated and 50μM H_2O_2 treated cells. Cells were synchronized using aphidicolin. (F) Western blot showing the expression pattern of cyclin B1 in untreated and 50μM H_2O_2 treated cells. Cells were synchronized using aphidicolin.

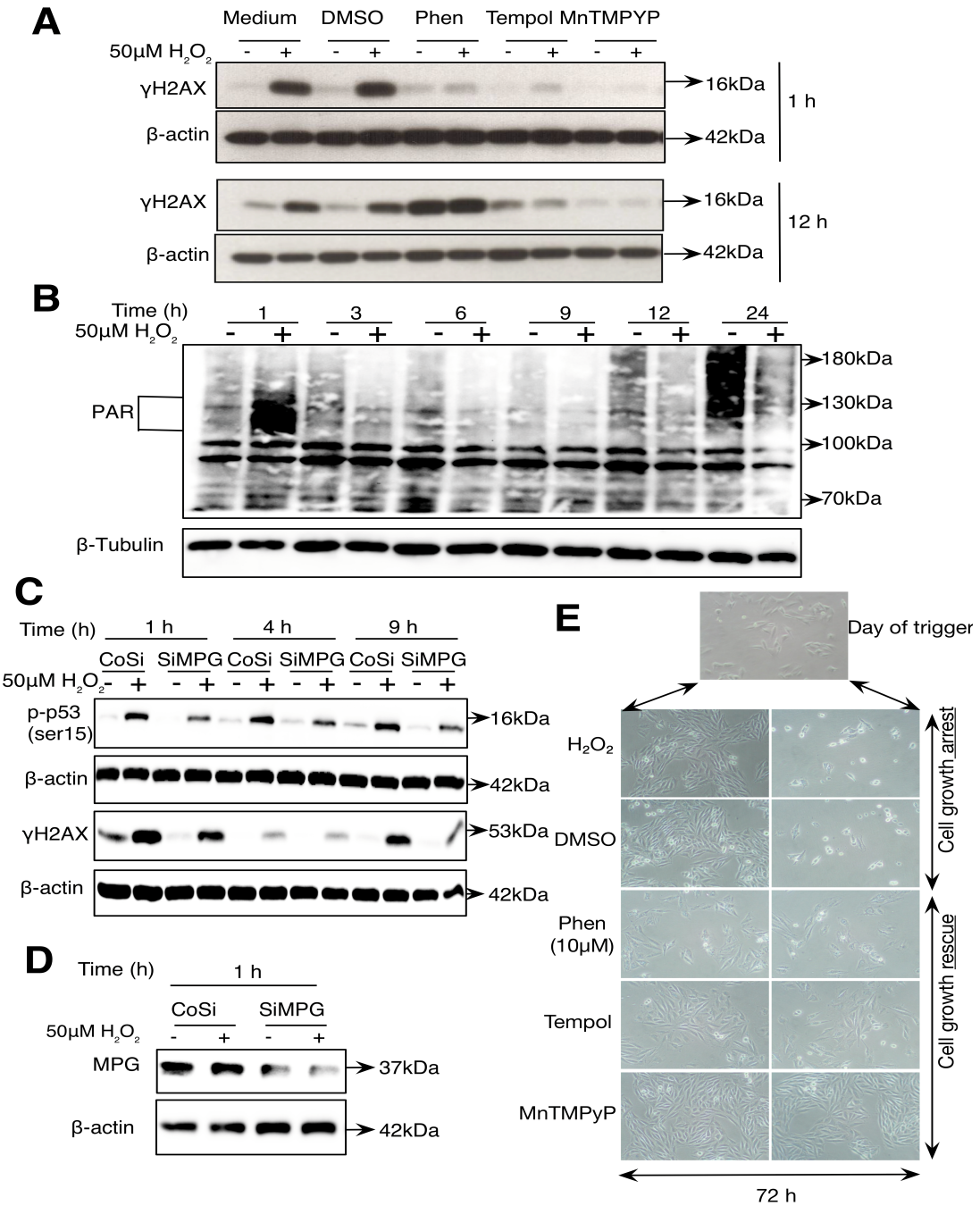

Supplementary Figure 2. First wave of DNA damage induced by sub-lethal oxidative stress involves Fe, PARP and MPG1 and is responsible for the induction of the second wave of DNA damage.
(A) L6 cells were pre-incubated for 2H with Fe chelators and co- incubated along with 50µM H_2O_2 for 1H and post-incubated only in the presence of the Fe chelator phenantroline and SOD mimetics, Tempol and MnTMPYP before assessing γH2AX. Western blot showing the kinetics of γH2AX in 50µM H_2O_2 treated cells measured at 1H and 12H in the presence of Fe chelators (Phen) and SOD mimetics (Tempol and MnTMPYP). The concentration of inhibitors used - Phen (10µM), Tempol (1mM) and MnTMPyP (100µM). The increase of γH2AX at 12H in the Phen treated control is due to the prolonged effect of Fe inhibition. Comparing the Phen treated control and 50µM H_2O_2 at 12H show similar levels of γH2AX. (B) Western blot detection of PAR in untreated and 50µM H_2O_2 treated synchronized cells using thymidine. (C) Western blot showing the levels of γH2AX and phosphorylated p53 (ser15) upon silencing of MPG1 at 1H, 4H and 9H post H_2O_2 treatment in the thymidine synchronized cells. (D) Western blot showing the levels of MPG1 at 1H post H_2O_2 treatment upon silencing with CoSi and SiMPG1. (E) Cell morphology pictures 72H after cells exposure to 50µM H_2O_2 in presence or absence of Phen, Tempol and MnTMPYP .

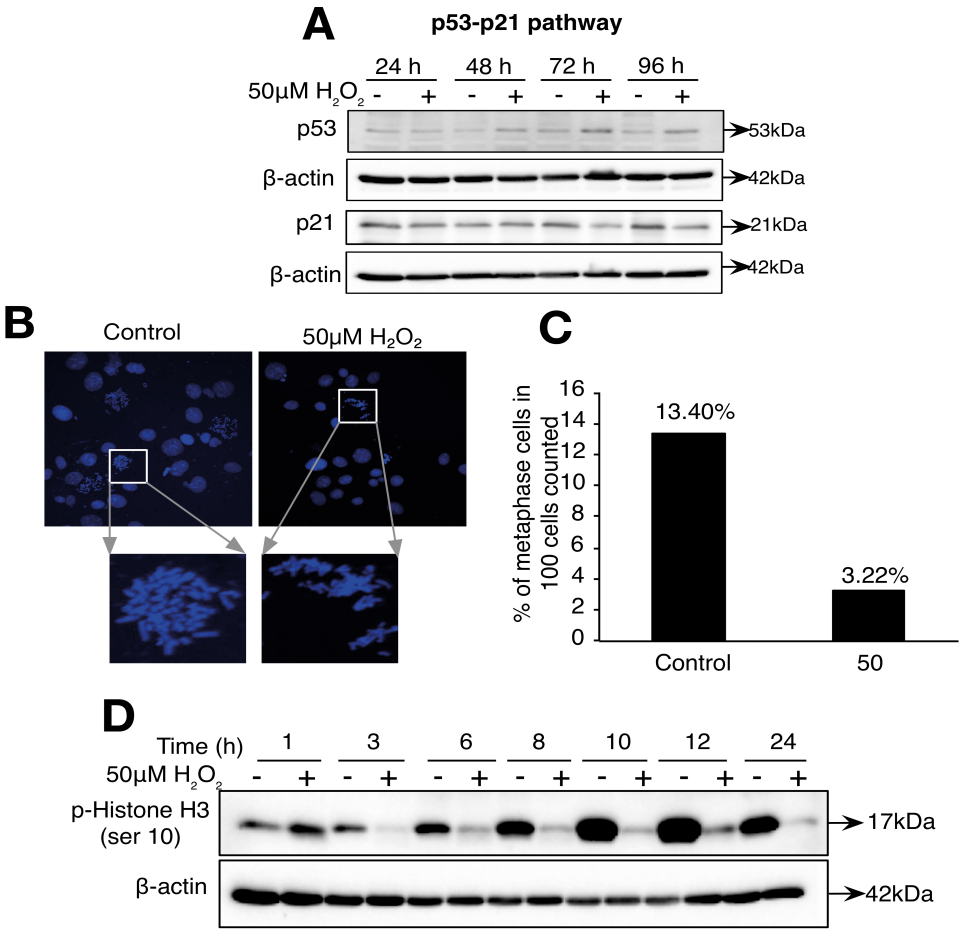

Supplementary Figure 3. Exposure of L6 cells to 50µM exogenous H_2O_2 did not engage p53-p21 pathway and H_2O_2 treated cells do not enter into mitosis.
Cells were synchronized in late G1 using thymidine before being treated with 50µM H_2O_2 for 1H. (A) Western blot showing the kinetics of total p53 and p21 at indicated

time points. (B) Metaphase chromosome spreads observed in untreated and 50μM H_2O_2 treated cells after 12H of H_2O_2 treatment. (C) Percentage of metaphase cells observed in untreated and 50μM H_2O_2 treated cells after 12H of H_2O_2 treatment. (D) Western blot analysis of p-Histone H3 (ser10) in untreated and H_2O_2 treated cells at indicated time points.

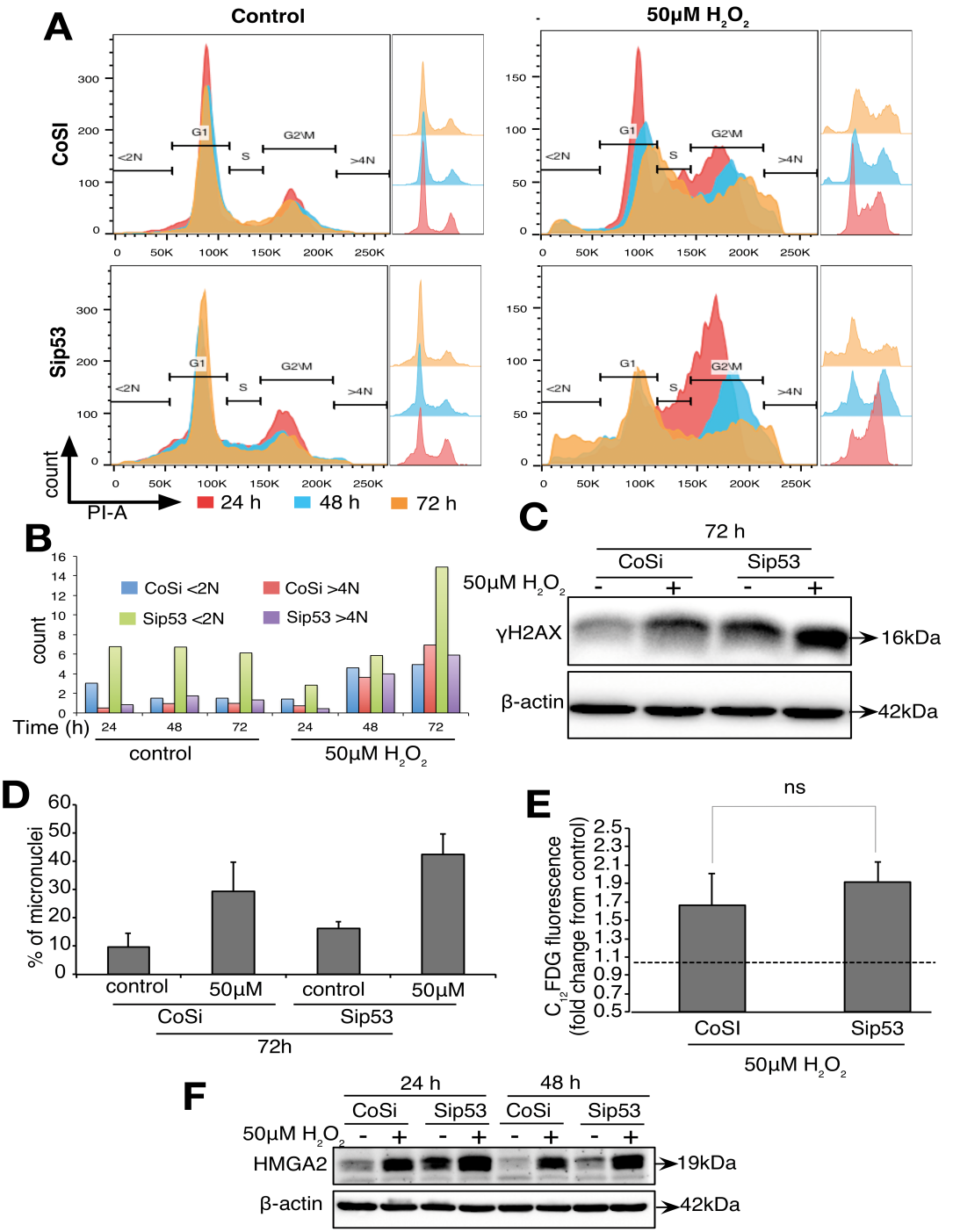

Supplementary Figure 4. Increased genomic instability and aneuploidy was observed upon abrogating cell cycle arrest by knocking-down p53.
Cells were synchronized with thymidine and then treated with 50μM H_2O_2 for 1H. (A) Cell cycle distribution showing the percentage of cells in each cell cycle phase in

untreated and 50µM H_2O_2 treated cells upon silencing with CoSi and Sip53. The cell population gating was fixed across all time points and it was based on the synchronized untreated-CoSi cell population. (B) Percentage of aneuploidy cells in CoSi -, Sip53 -untreated and H_2O_2 treated cells at indicated time points. (C) Western blot and densitometry plots showing γH2AX phosphorylation levels in CoSi -, Sip53 -untreated and H_2O_2 treated cells 72H after exposure to the oxidant. The densitometry data is the average of 3 independent experiments. (D) Percentage of micronucleated cells in CoSi-, Sip53- untreated and H_2O_2 treated cells at indicated time points. (E) C_{12}FDG staining measuring the SA-βgal activity in the untreated and 50µM H_2O_2 treated cells at 72H upon silencing with CoSi and Sip53. (F) Western blot showing HMGA2 expression at 24H and 48H upon silencing p53.

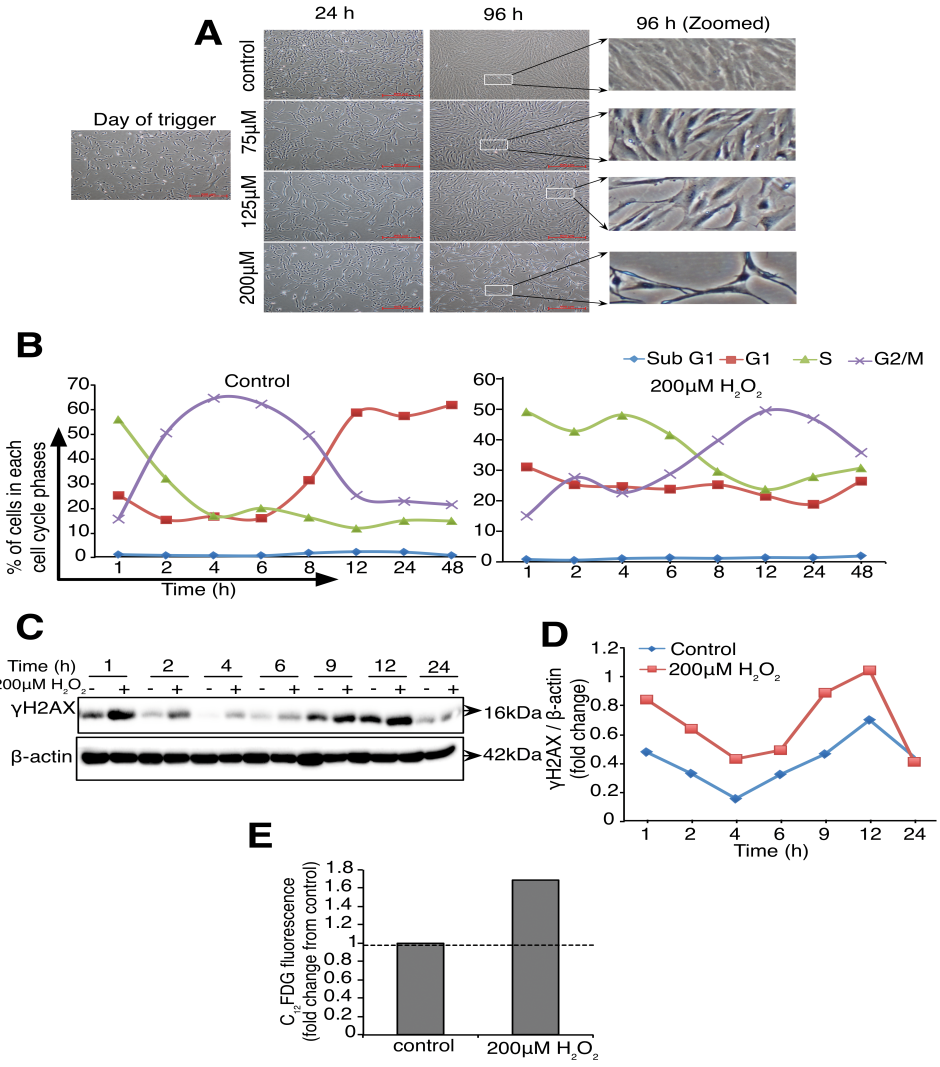

Supplementary Figure 5. Sub-lethal oxidative stress induces two waves of DNA damage is observed in RPE1 cells.

(A) Cell morphology of non-synchronized RPE1 cells treated with increasing concentration of H_2O_2 for 2H, observed using phase contrast microscope. Column 1: Cells after 24H of seeding and before H_2O_2 trigger. Column 2 and 3: Cell shape and morphology at 24H and 96H respectively. Column 4: Cell shape and cell morphology of RPE1 cells were zoomed and highlighted. (B) RPE1 cells were synchronized with thymidine and then treated with 200µM H_2O_2 for 2H. Line plots capturing the

percentage of cells in each cell cycle phase at the indicated time points. (C) Western blot showing the γH2AX profile at indicated time in the synchronized RPE1 cells treated with 200μM H_2O_2. (D) Graph showing the densitometry plots of γH2AX in control and 200μM H_2O_2 treated cells from (C). (E) C_{12}FDG staining measuring the SA-βgal activity at 72H in the synchronized untreated and H_2O_2 treated RPE1 cells.

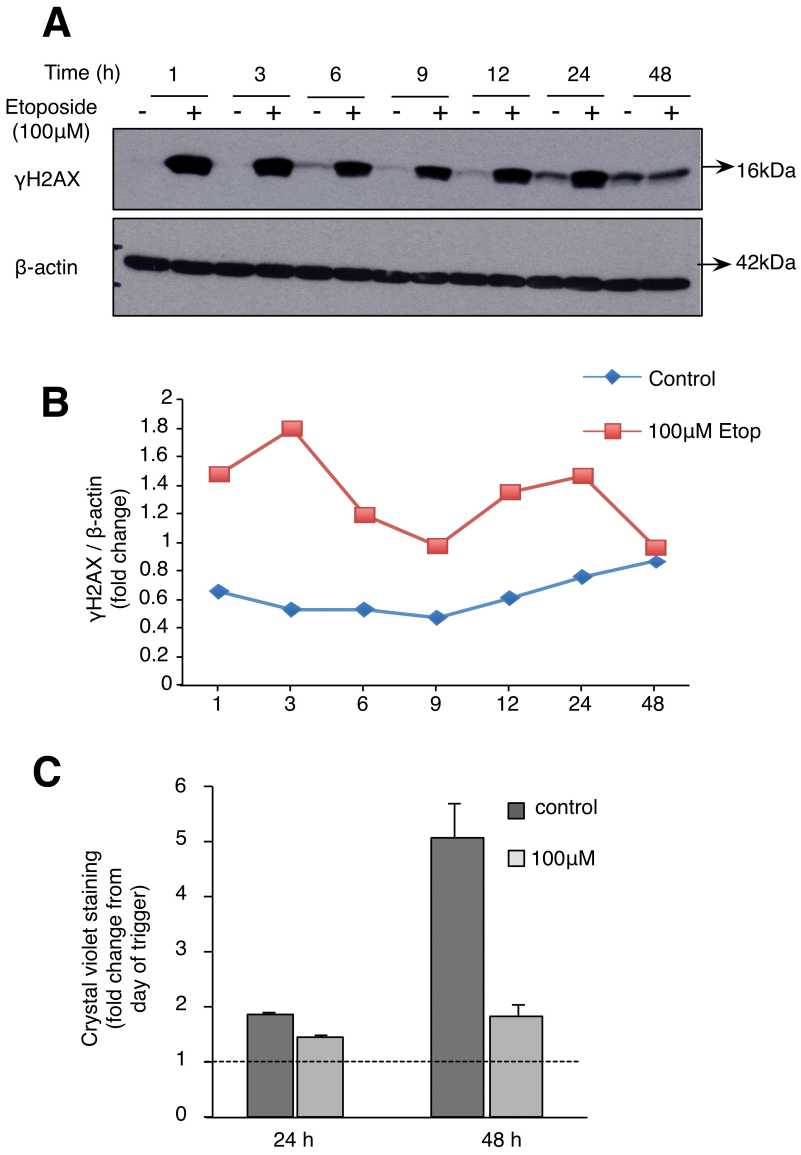

Supplementary Figure 6. Two waves of DNA damage are observed in L6 cells treated with etoposide.
(A) Western blot showing the γH2AX time kinetics in the non-synchronized L6 cells treated with etoposide (100μM). (B) Graph showing the densitometry plots of γH2AX in control and 100μM etoposide treated cells. (C) Cell density measured using crystal violet assay of non-synchronized L6 cells treated with 100μM etoposide for 2H.

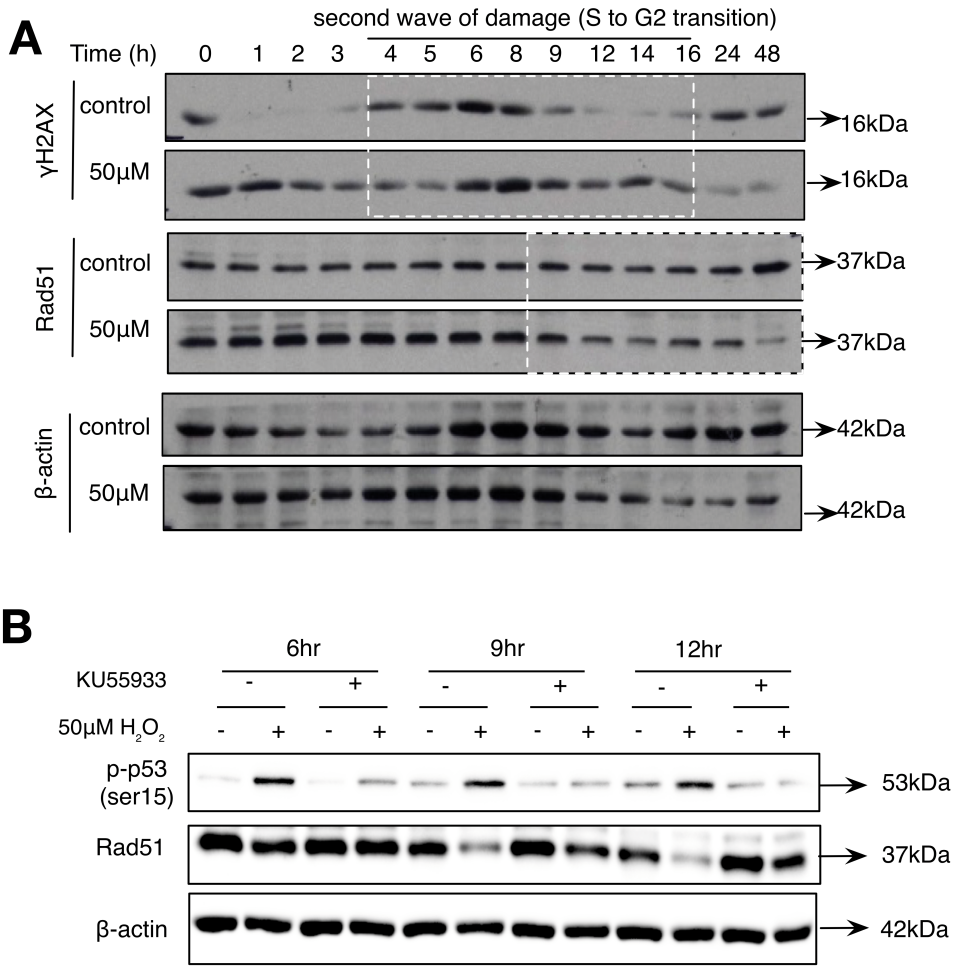

Supplementary Figure 7. Repression of Rad51 is downstream of second wave of DNA damage.

(A) Cells were synchronized with aphidicolin and then treated with 50μM H_2O_2 for 1H. Western blot showing the kinetics of γH2AX and Rad51 at indicated time points. The representative blots shown in Supplementary Figure 1D and Supplementary Figure 7A are from the same experiment. (B) Cells were synchronized with thymidine before being treated with 50μM H_2O_2 for 1H. Western blot showing the levels of Rad51 and phosphorylated p53 (ser15) after inhibition of ATM using KU55933 at the time of second wave of DNA damage (6 to 12H). KU55933 was added 3H after 50μM H_2O_2 treatment. The representative blots shown in Supplementary Figure 7B and Figure 3A are from the same experiment.

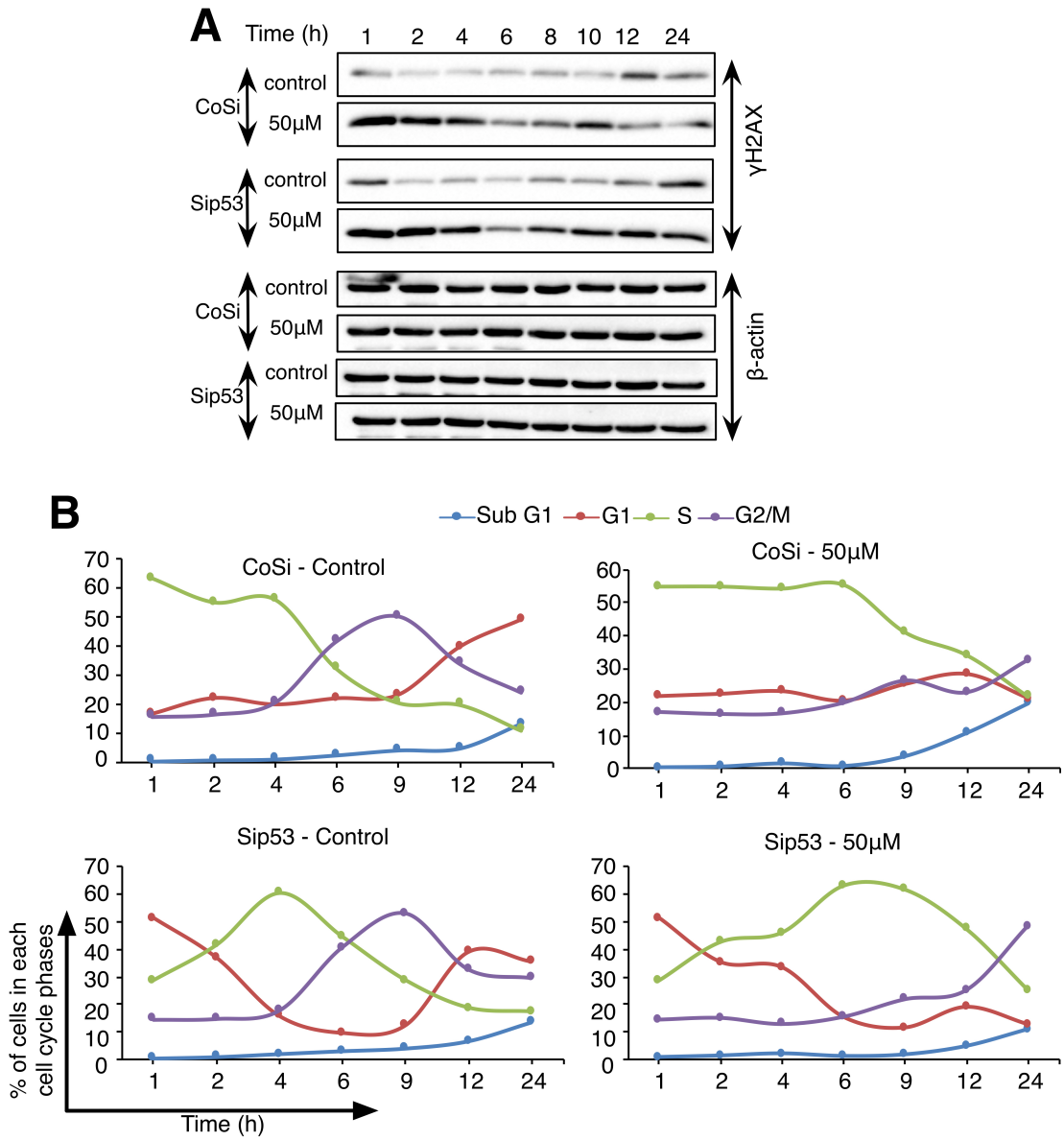

Supplementary Figure 8. Silencing p53 lead to prolonged S-phase delay and sustained second wave of DNA damage.

Cells were synchronized with thymidine and then treated with 50μM H_2O_2 for 1H. (A) Western blot showing the kinetics of γH2AX at indicated time points upon silencing with CoSi and Sip53. (B) Line plots capturing the percentage of cells in each cell cycle phase in untreated and 50μM H_2O_2 treated cells upon silencing with CoSi and Sip53 at the indicated time points. The representative blots shown in Supplementary Figure 8A and Figure 9A are from the same experiment.

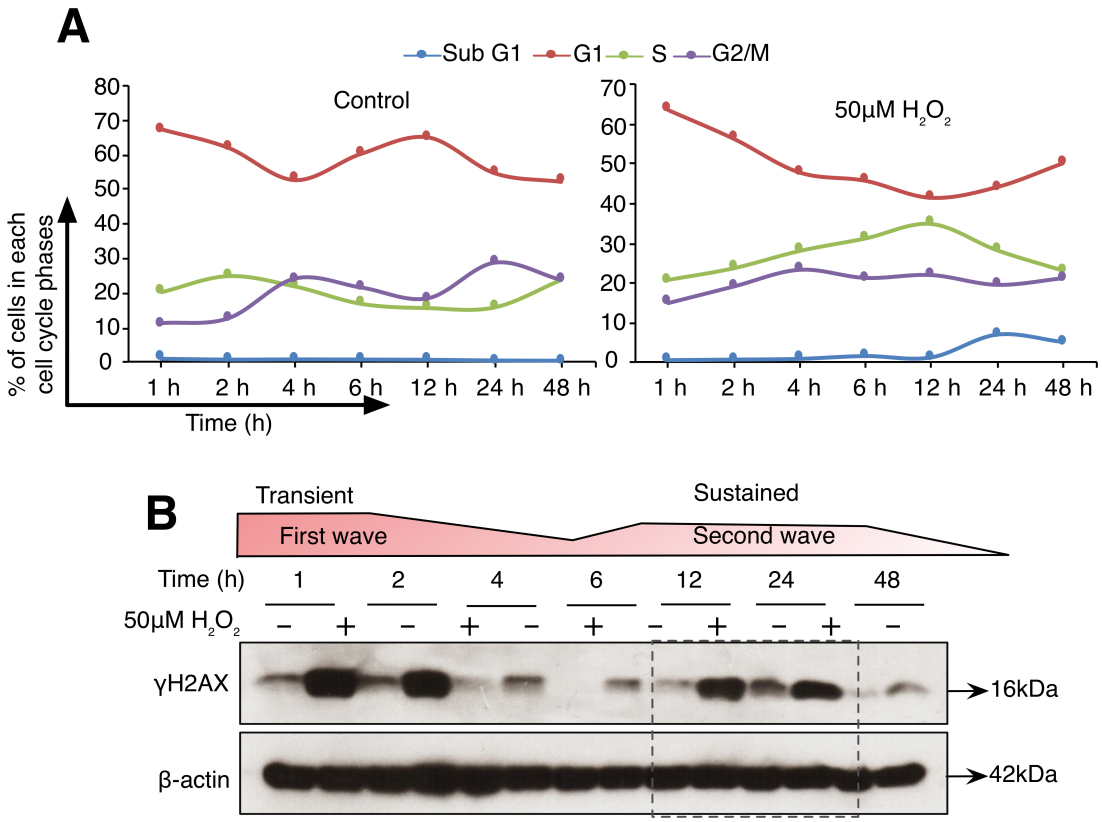

Supplementary Figure 9. Second wave of DNA damage is seen during the transition of cells from S and G2 phase of cell cycle in the non-synchronized L6 cells treated with sub-lethal dose of H_2O_2.

(A) Line plots capturing the percentage of cells in each cell cycle phase at the indicated time points in non-synchronized L6 cells treated with 50μM H_2O_2. (B) Western blot showing the γH2AX profile at indicated time in the non-synchronized L6 cells treated with 50μM H_2O_2.